2017

A Novel Method for Determination of Ammonium Isotope Ratios with Electrospray Ionization Mass Spectrometry

Rebecca J. Chmiel
Colby College

Recommended Citation

Chmiel, Rebecca J., "A Novel Method for Determination of Ammonium Isotope Ratios with Electrospray Ionization Mass Spectrometry" (2017). *Honors Theses.* Paper 947.
https://digitalcommons.colby.edu/honorstheses/947

A Novel Method for Determination of Ammonium Isotope Ratios with Electrospray Ionization Mass Spectrometry

Rebecca J. Chmiel
Environmental Studies Program
Colby College
Waterville, Maine

May 15, 2017

A thesis submitted to the faculty of the Environmental Studies Program in partial fulfillment of the graduation requirements for the Degree of Bachelor of Arts with honors in Environmental Studies

_____   _____   _____
Denise Bruesewitz, Adviser   D. Whitney King, Reader   Gail Carlson, Reader

ABSTRACT

Nitrogen (^{15}N) isotope tracer studies are an invaluable tool for understanding the rate of N transformations in the environment. A mechanistic understanding of N cycling is critical to management of excess N availability in freshwater and marine ecosystems. Conventional methods for measuring ^{15}N:^{14}N of dissolved inorganic nitrogen species are time consuming and require large sample volumes. Here, we present a technique for measuring ^{15}N:^{14}N in ammonium (NH_4^+) using electrospray ionization mass spectrometry (ESI-MS). NH_4^+ present in small volumes of sample (3 ml) is complexed with phenol via the Berthelot reaction, producing an indophenol complex (mass 198.05 or 199.05 amu) to increase the molar mass of the N species for mass spectrometry. Excess reagents are removed and the indophenol product concentrated using automated C-18 solid phase extraction. The extracts are run through a diode array UV-Vis detector to measure total NH_4^+ concentrations and then passed to the ESI-MS to obtain the ^{15}N:^{14}N of the complex. The low N concentration detection limits for ammonium (0.8 μM) coupled with quantitative isotope abundance determination allows for convenient, rapid characterization of N transformations in aquatic environments.

ACKNOWLEDGEMENTS

TABLE OF CONTENTS

INTRODUCTION

The biogeochemical conversion of nitrogen (N) through the environment via the nitrogen cycle is a fundamental driver of ecosystem productivity, diversity, and function (Vitousek et al. 1997). The N cycle is primarily driven by microorganisms that undergo processes such as nitrification and nitrogen fixation that transform N species such as nitrate (NO_3^-), ammonium (NH_4^+), and N_2 gas (Figure 1). The largest pool of N on earth, the N_2 gas that makes up 78% of the atmosphere, is not able to be utilized by most organisms; N_2 gas is only bioavailable to specific N-fixing bacteria that are able to break the strong triple N≡N bond (Delwiche 1977). However, the development of the Haber-Bosch process in the early twentieth century allowed for the artificial fixation of N_2 gas into ammonia (NH_3):

$$N_2 + 3H_2 \rightarrow 2NH_3$$
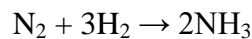
(Glibert et al. 2014). The development of this process paved the way for large-scale artificial fertilizer use in the latter half of the twentieth century, increasing the global bioavailable N in terrestrial, marine, and freshwater ecosystems (Glibert et al. 2006). Human activities such as fertilizer use and fossil fuel combustion (releasing N_2O, a greenhouse gas, into the atmosphere) have heavily altered the global reactive N pool (Vitousek et al. 1997, Dodds et al. 2002, Alexander et al. 2008), making alteration of the N cycle one of the starkest elements of anthropogenic change (Rockstrom et al. 2009).

Much of the N introduced into the environment, whether via agricultural use, fossil fuel combustion, or other processes, eventually finds its way to streams, lakes, rivers, and oceans (Howarth et al. 1996, Galloway et al. 2003, Bruesewitz et al. 2012). The increase of bioavailable N in aquatic environments creates an increase in ecosystem primary productivity which in turn leads to a multitude of problems, including the development of hypoxic zones (Rabalais et al. 2002, Diaz and Rosenberg 2008), enhancing conditions for harmful algal blooms (Carpenter et al. 1998, Glibert et al. 2014, Paerl et al. 2016), and decreasing drinking water quality (Spalding and Exner 1993, Nolan et al. 1997, Rupert 2008).

In light of anthropogenic changes in N availability, there is an ongoing need to refine our understanding of N transformations in freshwater and marine ecosystems so we can
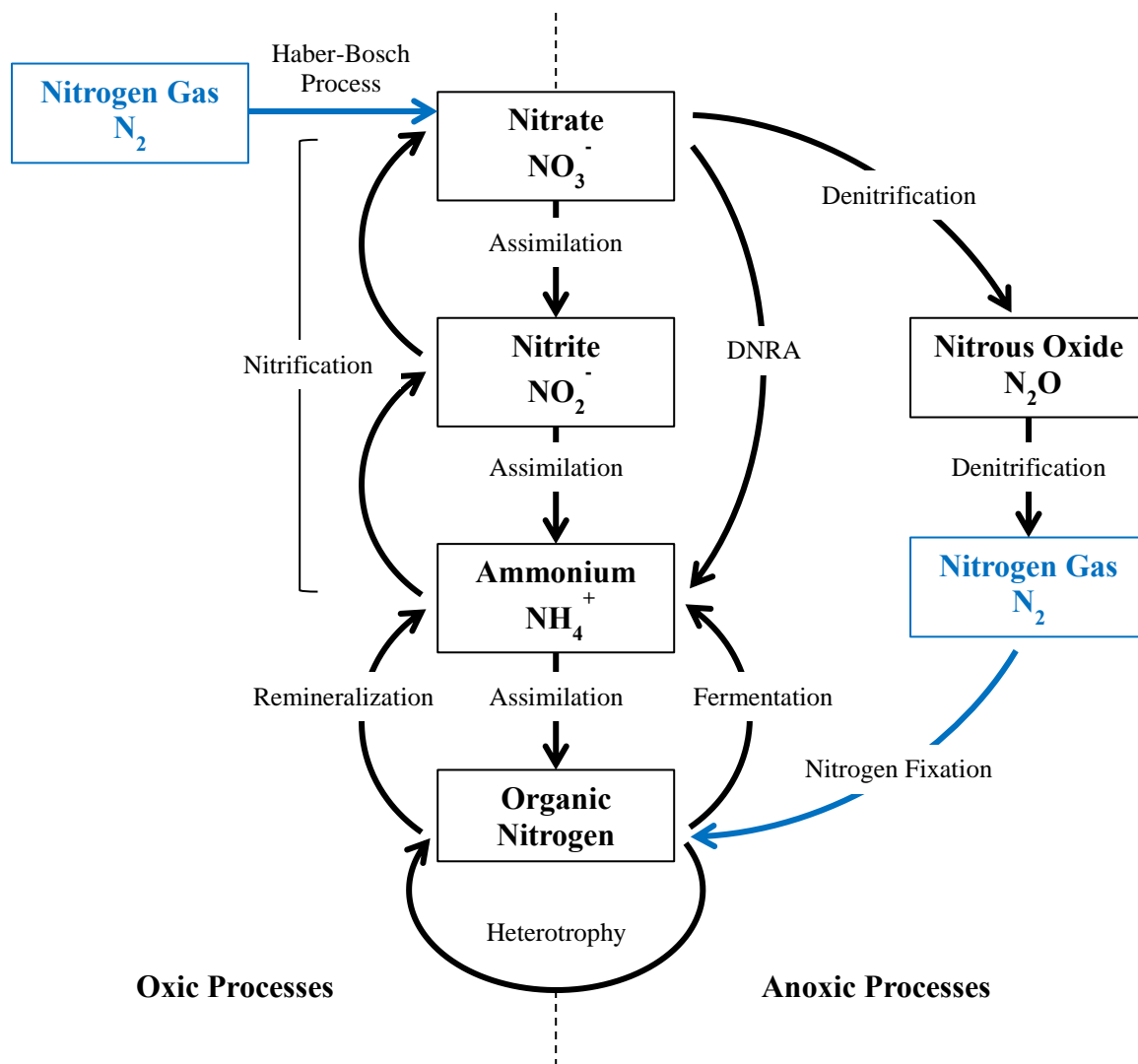
Figure 1. Common transformations that make up the N cycle. Processes are separated by oxic transformations on the left, which require oxygen to proceed, and anoxic transformations on the right, which do not require oxygen. Processes shown in blue are N fixation reactions that transform N_2 gas into a bioavailable form of N, either via N-fixing bacteria (anoxic) or the artificial Haber-Bosch process (oxic). Adapted from Dodds et al. 2002.

better predict the effect of N perturbations on a system (Peterson et al. 2001, Alexander et al. 2009, Wymore et al. 2016). However, direct measurement of N transformations is difficult because multiple cycling processes take place concurrently (Groffman et al. 2006, Burgin and Hamilton 2007). Instead, N isotope tracers are used to determine rates of N cycle transformations.

Isotopic tracer studies of ecosystems or mesocosms are a powerful tool to quantify N transformations in a system through the addition of ^{15}N, possibly in the form of $^{15}N\text{-}NH_4^+$

or ^{15}N-NO$_3^-$. Often, the ^{15}N tracer is experimentally added to a system such as a soil core or a water column, and the rate at which the ^{15}N is transformed into another N species by biotic and abiotic processes allows researchers to determine the rate of the N cycling process. This experimental technique can be used to calculate many N transformation rates, including nitrification (Carini and Joye 2008), denitrification (McCarthy et al. 2015), dissimilatory nitrate reduction to ammonium (DNRA) (Burgin and Hamilton 2007) and assimilation, or N uptake (Gardner et al. 2006, Carini and Joye 2008, Bruesewitz et al. 2015).

After these ^{15}N tracer addition experiments are completed, the amount of ^{15}N present in a collected sample must be determined. Specifically, the concentration of total N present and the isotopic ratio of ^{15}N present (relative to ^{14}N) within the sample must be quantified. In this paper, we specifically discuss the quantification of ^{15}N-NH$_4^+$ species from such experiments.

Different methods can be used to determine NH$_4^+$ isotope ratios from N tracer experiments (Table 1), many of which first convert NH$_4^+$ into another N species before instrumental analysis. Steam distillation methods (Velinsky et al. 1989) and NH$_3$ diffusion methods (Brooks et al. 1989, Sorensen and Jensen 1991, Holmes et al. 1998) convert NH$_4^+$ to gaseous NH$_3$ for analysis by isotope ratio mass spectrometry (IRMS). These older techniques can be laborious and time-consuming, often demanding large volumes of each water sample to achieve a low detection limit. Another technique, ammonium isotope retention time shift (AIRTS) via high performance liquid chromatography (HPLC) (Gardner et al. 1991, 1995), has minimal sample preparation, small sample volume, a low detection limit, and is well-automated. However, sample throughput on the HPLC is slow (~2.7 hr/sample), making it difficult to process a high throughput of samples. Additional methods convert ammonium to other species, including N$_2$O gas (Zhang et al. 2007, Liu et al. 2014), 1- sulfonato-*iso*-indole (Johnston et al. 2003), and N$_2$ gas (Strange et al. 2007).

Conversion of NH$_4^+$ to indophenol via the Berthelot reaction can also be used to quantify ^{15}N-NH$_4^+$. Indophenol is typically a blue dye containing one N atom, and the Berthelot reaction is a standard method used to determine NH$_4^+$ concentration using UV-

Table 1: Selected references for $^{15}N-NH_4^+$ determination methods. In absence of a stated $[NH_4^+]$ limit of detection, the value of the lowest sample explicitly analyzed was used. For some methods, mass units are more appropriate than concentration units and are reported for the lowest $[NH_4^+]$ analyzed. Citation information was determined by Scopus on December 22, 2016.

Selected Reference	Sample Preparation	Instrument	Sample Volume	$[NH_4^+]$ Limit of Detection	Cited by
Brooks et al., 1989	$NH_4^+ \rightarrow NH_3$; "Ammonia Diffusion"	Automated NaOBr MS; Direct Combustion MS	--	50 μg N	476
Holmes et al., 1998	$NH_4^+ \rightarrow NH_3$; "Ammonia Diffusion"	IRMS	4 L	0.5 μM	207
Gardner et al., 1995	Direct NH_4^+ Injection	AIRTS/HPLC*	3 mL	0.2 μM	49
Zhang et al., 2007	$NH_4^+ \rightarrow N_2O$	PT-CF-IRMS**	20 mL	0.5 μM	35
Strange et al., 2007	$NH_4^+ \rightarrow N_2$	SPINMAS***	5 mL	10 μg N	34
Dudek et al., 1986	$NH_4^+ \rightarrow$ Indophenol; "Solvent Extraction"	Emission Spectrophotometer	400 mL	--	33
Preston et al., 1996	$NH_4^+ \rightarrow$ Indophenol; "Solid Phase Extraction"	GC/MS	2 L	--	14
This Method	$NH_4^+ \rightarrow$ Indophenol; "Solid Phase Extraction"	ESI-MS	3 mL	0.8 μM	--

*Ammonium Isotope Retention Time Shift/High performance liquid chromatographer
**Purge-and-trap continuous flow isotope ratio mass spectrometer
***Sample preparation unit for inorganic nitrogen (SPIN) with IRMS or quadrupole MS

Vis spectroscopy (Solorzano 1969, Patton and Crouch 1977). The NH_4^+ must first be converted to NH_3 in a basic solution before the reaction proceeds. The Berthelot reaction is selective for NH_3 specifically, so other amines present in the sample will not be reacted, such as amines in dissolved organic carbon (DOC) or proteins. The absorbance of the indophenol created can then be used to quantify total NH_3 concentration.

The strong color of the dye is due to the molecule's conjugated π-bond system, which absorbs at the $\pi \rightarrow \pi^*$ transition. Indophenol has two predominant protonation states: a deprotonated state, characterized by a dark blue color that absorbs at 628 nm, and a protonated state, characterized by a pale red/pink color that absorbs at 495 nm. The pKa of indophenol was previously calculated to be 7.8 (Z. Mondschein, personal communication). Refer to appendix for indophenol absorbance spectra (Figure A.1).

The use of indophenol formation from NH_4^+/NH_3 can be extended from the determination of total NH_3 concertation to the quantification of ^{15}N-NH_4^+ isotopic ratios. The synthesis of a larger molecule, such as indophenol, from NH_4^+ is necessary for isotopic analysis on many mass spectrometers to increase the analyte molecule's mass to be within the mass range of the instrument. The high concentration of N species in most isotope tracer studies and widespread use of the reaction for concentration determination makes the formation of indophenol a convenient technique to prepare samples for NH_4^+ isotopic tracer study.

Previous indophenol methods for isotopic characterization have used solvent extraction with analysis by emission spectroscopy (Dudek et al. 1986) and solid phase extraction with analysis by gas chromatography mass spectrometry (GC/MS) (Preston et al. 1996, Clark et al. 2006). The GC/MS method in particular is precise and highly accessible due to the wide availability of GC/MS instruments. However, the solid-phase extraction process requires significant time for sample processing and large sample volumes (2 L).

We present a new method for simultaneous total NH_3 (NH_3 and NH_4^+) concentration and isotopic ratio determination for N tracer studies using semi-automated solid-phase extraction (SASE) and mass spectrometry with electrospray ionization input (ESI-MS). Water samples from ^{15}N tracer experiments were reacted to produce indophenol (Solorzano 1969). The solutions were extracted by C-18 column chromatography to

remove excess reactants and produce a stable, concentrated sample for MS analysis. Samples were then analyzed with a combined spectrophotometer for total NH_3 concentration and ESI-MS for ^{15}N:^{14}N, expanding the toolbox for analysis of N isotope studies to ESI-MS instruments. Finally, we apply this method to analyze the results of a ^{15}N isotopic tracer experiment to examine rates of DNRA in sediment cores from the Mission River, TX.

This novel method is semi-automated, uses small sample volumes, has a low limit of detection, and is easily adjustable. It can be utilized with water samples of various matrixes, including saltwater and water containing DOC, which allows for a range of sample types that can be processed. The use of this technique will expand the ability of N researchers to preform and analyze ^{15}N tracer experiments in a convenient manner. This method improves our capacity to quantify N cycle transformations in natural and human-impacted systems by allowing for easier analysis of ^{15}N tracer experiments.

METHODS

For this novel method, we developed and optimized a protocol for simultaneous total NH_3 (NH_3 and NH_4^+) concentration and isotopic ratio determination for ^{15}N-NH_4^+ tracer studies. The steps for this technique include (1) color formation to generate indophenol from total NH_3, (2) extraction to purify and concentrate the indophenol sample, (3) instrumental analysis on the UV-Vis spectrophotometer and ESI-MS, and (4) data analysis (Figure 2).

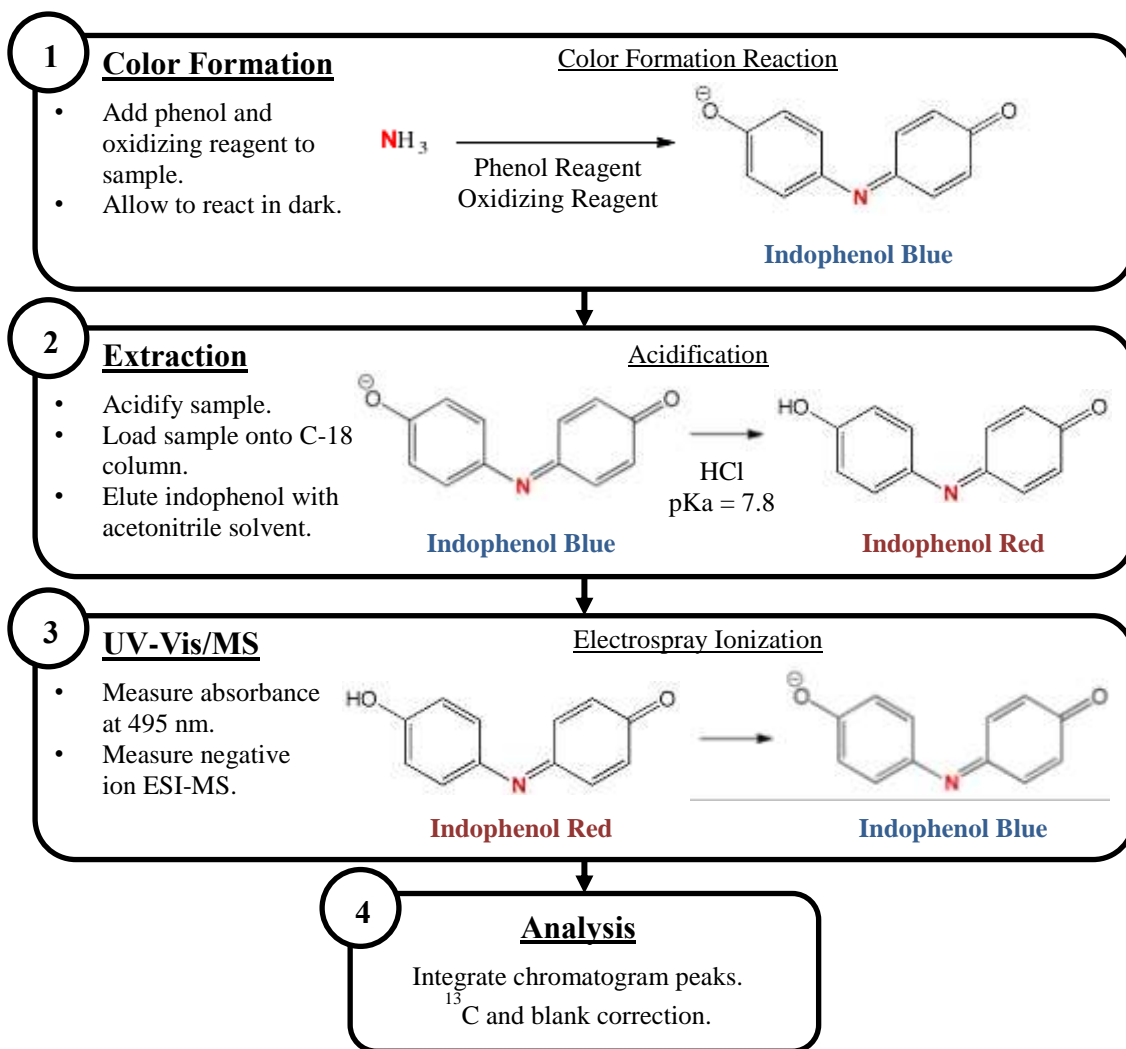Figure 2. Summary of NH_4^+ analysis protocol. (1) Total NH_3 is bound into indophenol blue. (2) Acidification protonates the indophenol and optimizes the extraction process. Extraction removes excess reagents and concentrates the sample. (3) Samples are run on a diode array detector (DAD) spectrophotometer and a mass spectrometer with an ESI input. (4) Mass peaks are integrated at 198.06, 199.06, and 200.06 m/z.

Color Formation

NH$_4^+$ was deprotonated in a basic reagent solution to form NH$_3$, and then complexed into indophenol dye (Solorzano, 1969) to increase the mass of the N species, allowing it to be easily ionized and detectible on most mass spectrometers. Refer to appendix for full reaction (Figure A.2). The indophenol molecule displays a blue coloring in its deprotonated form and a red/pink color in its protonated form (pKa = 7.8). The predicted mass-to-charge (m/z) spectrum of the indophenol ion (-1 charge) is 198.06 (100%) m/z and 199.06 (13.0%) m/z at natural abundance of N isotopes.

All glassware used in the color formation procedure was washed in 20% hydrochloric acid before use. All chemicals used for reagent and standard preparation were obtained from Sigma Aldrich unless otherwise stated.

A standard calibration curve was prepared using ^{14}N-NH$_4$Cl and ^{15}N-NH$_4$Cl that incorporates both varied N concentrations and isotopic ratios into a single set of standards. Suggested standards for the calibration curve (Table 2) include a reagent blank and two high NH$_4^+$ concentration standards, one with 0% ^{15}N and one with 100% ^{15}N, to monitor any irregularities in the ^{14}N-NH$_4$Cl and ^{15}N-NH$_4$Cl standards. Standards (3 mL) were prepared in duplicate by mass in 10 mL glass vials using stock solutions of 1.0 mM NH$_4$Cl (natural abundance = 99.6% ^{14}N) and 1.0 mM ^{15}N-NH$_4$Cl (98% purity).

A phenol reagent was prepared with 0.37 M phenol and 1.5 mM sodium nitroprusside in milli-Q water. An oxidizing reagent was prepared with two components: a citrate buffer and sodium hypochlorite (available chlorine 4.00-4.99%). The citrate buffer (pH

Table 2. Suggested NH$_4$Cl standards used for both concentration and isotopic ratio determination.

Total NH$_4^+$ (μM)	%^{15}N-NH$_4^+$
0	0
5	20
10	40
20	60
35	80
50	0
50	100

12.9) was prepared with 0.39 M sodium citrate and 0.25 M sodium hydroxide in milli-Q water. The citrate buffer and the sodium hypochlorite were combined respectively in a 4:1 ratio to form the oxidizing reagent, which must be prepared just prior to analysis. Formation of indophenol requires deprotonation of NH_4^+ to NH_3, which occurs in the basic solution created by the oxidizing reagent (Solorzano 1969).

Samples and standards (3 mL) were complexed by adding 115 µL of the phenol reagent, briefly shaking the sample, adding 115 µL of the oxidizing reagent, briefly shaking the sample, and reacting in the dark to prevent degradation. Samples were allowed to react for 6-24 hours for indophenol formation. Then, 81 µL of 0.625 M HCl was added to each sample. The acid protonates the indophenol molecule, forming the red/pink conjugate acid of indophenol, ending the reaction and optimizing the complex for solid-phase extraction.

Solid-Phase Extraction

Sequential solid-phase extraction removed excess inorganic reagents after color formation and concentrated the sample to 1 mL for analysis. Extraction was performed within 8 hours of acid addition on a Semi-Automatic Solid-phase Extractor (SASE), which consisted of a 10 mL Tecan Syringe, 2 C-18 Sep-Pak light columns (Waters) placed end-to-end to minimize indophenol leaking, and a Valco A/B valve, all controlled by LabView software (Figure 3). LabView software uses an intuitive visual programing language to create personalized "dashboards" for automated systems like SASE. The syringe withdrew inputs and directed them into the column, while the A/B valve allowed for the control of outputs, with indophenol directed to sample vials (A) and excess reagents directed to waste (B).

The elution procedure for the sequential solid-phase extraction of protonated indophenol (Table 3) began with a priming step. The C-18 Sep-Pak columns were rinsed with acetonitrile by the Tecan syringe before output tubing was connected between the columns and the A/B valve. The acetonitrile rinsed the columns of loose C-18 particles that could clog the valve. The columns were used for a maximum of 20 sample elutions before they were replaced and the priming step was repeated.

Solvent

Milli-Q Water

Sample/Rinse

C-18 Sep-Pak
Columns

A/B Valco
Valve

A. Sample
To DAD
and ESI-MS

B. Waste
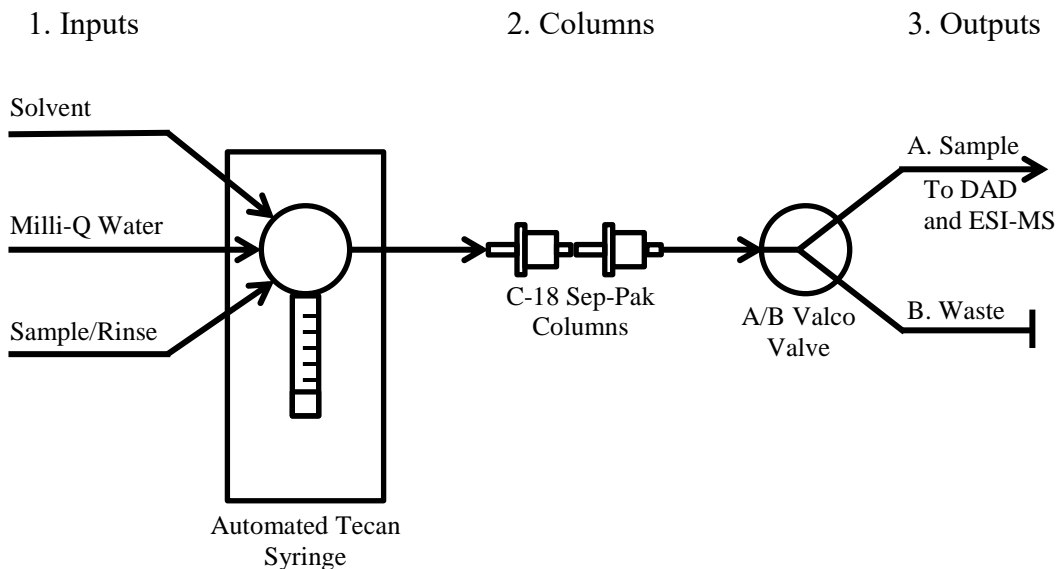
Automated Tecan
Syringe

Figure 3. Conceptual diagram of SASE used for indophenol reduction. (1) Inputs are pumped into the system via a Tecan syringe, controlled by LabView software. (2) Two C-18 columns are connected by tubing to the syringe and the A/B valve. Indophenol is loaded onto the columns in aqueous solution and eluted off the columns in acetonitrile solvent. (3) Outputs are separated by the A/B valve into sample (A) and waste (B). The sample is collected into a 1 mL amber glass vial for analysis on the DAD and ESI-MS.

An initial water rinse optimized the C-18 columns for organic indophenol retention. The acidified sample was then loaded onto the columns, and the red/pink color was visibly retained on the columns in high concentration samples. The inorganic portion of the sample that was not retained on the columns was directed to waste. This step can be scaled to any desired sample volume, as long as the indophenol does not exceed the capacity of the columns. Acetonitrile was pumped through the columns to elute the indophenol off the C-18 and into a 1 mL amber vial for MS analysis. Rinse steps were liberally used throughout the extraction procedure to wash the column and prevent cross-contamination of samples.

Analysis on ESI-MS

Samples were analyzed on an Agilent G6230A time-of-flight mass spectrometer with an electrospray ionization input (ESI-TOF-MS) and a paired diode array detector (DAD) to give simultaneous absorbance spectra. A TOF-MS was selected for its high resolution, but the specific instrument is not required for this technique. Other MS types

Table 3. Sequential solid-phase extraction of indophenol on SASE. A and B outputs refer to the A/B valve positions; A directs column output to the sample output tubing and B directs column output to the waste output tubing. Solvent used is 100% reagent-grade acetonitrile. Rinse steps help to prevent contamination of the previous sample.

Step	Purpose	Input	Volume (mL)	Output	Notes
1	Priming	Solvent	4	--	No output tubing connected to column. Repeated only when columns are replaced.
2	Rinse	Solvent	4	B	Column and tubing rinse.
3	Rinse	Solvent	1	A	Output A tubing rinse. Do not keep as sample.
4	Rinse	Sample*	2	Sample Input	To rinse sample input tubing, milli-Q water was withdrawn through the sample input and dispelled through the same input to waste.
5	C-18 Optimization	Milli-Q	3	B	For maximum indophenol retention on C-18 columns.
6	Sample Loading	Sample	3	B	Removal of inorganic components in sample and retention of indophenol on columns.
7	Rinse	Milli-Q	3	B	Column rinse.
8	Purging Sample Tubing	Solvent	1	B	To being eluting indophenol off columns while purging output tubing of excess liquid. Volume is dependent on the length of output tubing.
9	Sample Elution	Solvent	1	A	Sample collected in amber vial for instrumental analysis.

*Step 4 is a rinse of the sample input tubing with milli-Q water (18 MΩ), not with actual sample.

can be used as long as they are compatible with an ESI input or a similar ionization technique. Each sample (10 µL) was injected with an acetonitrile solvent at a flow rate of 0.400 mL min^{-1} and run for 6 min with a 1 min post-time rinse. The ESI-TOF-MS was run on negative ion mode with a data acquisition rate of 2 spectra s^{-1}. Additional parameters for ESI-TOF instrumentation are given in Table 4.

A peak at 495 nm with a 10 nm bandwidth was extracted from the DAD and integrated to find peak area. A calibration curve of $[NH_4^+]$ vs. absorbance peak area was generated for unknown analysis. Peak chromatographs from the mass spectrometer were extracted from 198.03-198.10 m/z and 199.03-199.10 m/z, and were integrated to calculate peak area. A correction for the blank was applied by subtracting the blank peak areas from each standard peak area. A correction for the carbon-13 (^{13}C) isotope is necessary because abundance of ^{13}C is ~1.1% in the environment. In other words, ~1.1% of the C atoms in the indophenol sample are an isotopically heavy version of C. This signal would interfere with the ^{15}N isotope signature, and must be predicted and corrected for. A ^{13}C correction was applied to the peak areas by decreasing the 199 m/z peak area (A_{199}) by 13.0% of the 198 m/z peak area (A_{198}) to find the corrected 199 m/z peak area (A^*_{199}):

$$A^*_{199} = A_{199} - (A_{198} \times 0.130) \qquad (1)$$

The correction of 13.0% is the expected percentage of indophenol molecules containing one ^{13}C atom, as predicted by ChemDraw (v. 16.0.0.82).

Table 4. Empirically optimized ESI-TOF parameters.

Parameter	Value
Nebulizer Gas Temperature	200°C
Drying Gas Rate	6 L min^{-1}
Nebulizer Pressure	20 psig
Sheath Gas Temperature	200°C
Sheath Gas Flow Rate	12 L min^{-1}
Cap Voltage	1500 V
Nozzle Voltage	500 V
Fragmentor Voltage	200 V
Skimmer Voltage	65 V

%^{15}N was determined by the 198:199 m/z corrected peak area ratio:

$$\%\,^{15}\text{N} = A^{*}_{199} / (A_{198} + A^{*}_{199}) \times 100 \quad (2)$$

A calibration curve of calculated %^{15}N vs. standard %^{15}N was generated for unknown analysis. Limits of Detection (LOD) for both concentration and %^{15}N calibration curves were calculated from the slope (m) and the mean standard deviation of a low-concentration sample (S_y); (Harris 2010).

$$LOD = 3 \times (S_y / m) \quad (3)$$

Effect of Analysis Time

To test how long samples could remain in the color formation reaction before acidification and extraction, the time before acidification was varied. Replicates of a calibration curve were allowed to react for 6 hours, 1 day, 3 days, and 1 week. The effects on the calibration curves were analyzed to determine how long a sample can stay in the color formation stage of the process and the effect of degradation on the indophenol dye during the color formation reaction.

In order to test the stability of samples after extraction in acetonitrile, the same calibration curve was continually analyzed on the DAD and ESI-MS for 1 month. This allowed for an estimation of how long extracted samples could be stored in acetonitrile solvent before instrumental analysis without degradation.

DOC and Salinity Effects

Many environmental studies to determine N transformation rates are conducted in saltwater ecosystems or ecosystems with some amount of DOC. To determine if this method can be applied to samples at salinity or with DOC, a range of spikes of a known concentration and isotopic ratio were added to water with 6.69±0.08 mg DOC L^{-1} from a stream in Oakland, Maine and filtered seawater at 36‰ salinity from the Damariscotta Estuary in Maine. The variance and slopes of the spike responses were analyzed.

Application to Environmental Samples

To demonstrate the application of this novel method for the analysis of environmental ^{15}N tracer experiments, we conducted a sediment core incubation

experiment to quantify rates of NO_3^- transformation to NH_4^+ via DNRA. Sediment cores and carboys of sub-surface water were collected in duplicate from upstream and downstream sites along the Mission River, Texas in January, 2017 (Figure 4). The cores were incubated at 12°C with 5 cm of water above the sediment, a cross-sectional area of 0.0045 m^2, and a continuous water flow of 1.0-1.3 mL min^{-1}. Inflow and outflow water from the sediment core incubations was sampled 24 h and 48 h after field collection. The incubation water was then lowered to 15 L and spiked with $Na^{15}NO_3^-$ (Cambridge Isotope Laboratories, >98% ^{15}N) to give a concentration of 25 μM ^{15}N. Inflow and outflow water from the sediment core incubations was sampled 24 h, 48 h, and 72 h after the ^{15}N-NO_3^- spike. Water samples were filtered with a 0.45 μm polyethersulfone (PES) membrane filter (Whatman), and stored frozen.
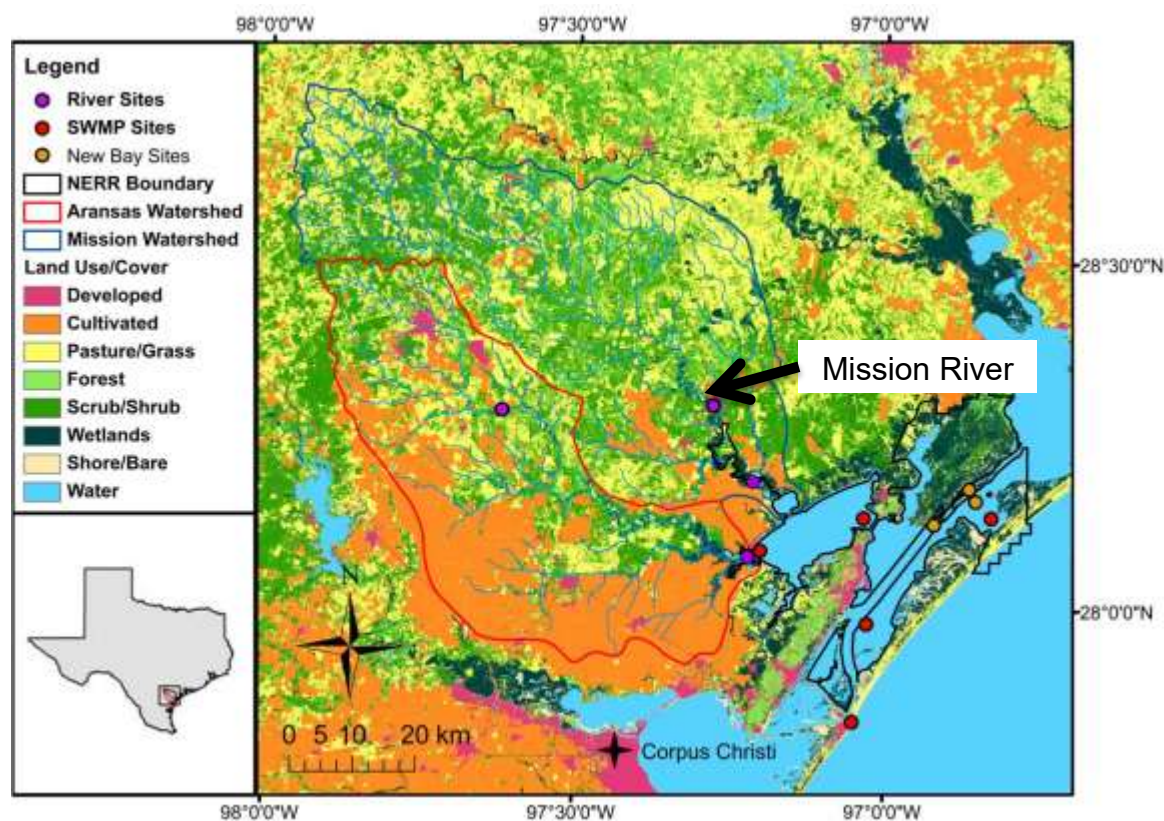

Figure 4. Map of the Mission River study site in southern Texas with land use and land cover types given. The Mission River watershed is outlined in blue. Specific points marked on this map are unrelated to the study presented here. From Mooney and McClelland (2012).

14

Upon thawing, 3 mL of each sample was analyzed for total NH_3 concentration and $\%\,^{15}N\text{-}NH_4^+$, as described above. For the input and the output water samples, the total $[NH_4^+]$ was determined from the concentration calibration curve and the $\%\,^{15}N\text{-}NH_4^+$ was determined by Equation 2. The net N flux of the system was calculated with the NH_4^+ concentration of the output water ($[Out]$) and input water ($[In]$) in μM, the cross-sectional area of the soil core (A_{core}) in units of m^2, and the flow rate of the input and output water (F) in mL min^{-1}:

$$\text{Flux} = (F / A_{core}) \times ([Out] - [In]) \times 0.06 \qquad (4)$$

The factor of 0.06 is a unit conversion factor, and the flux is in units of $\mu mol\ N\ m^{-2}\ h^{-1}$. When the net NH_4^+ flux is positive, the system displays net NH_4^+ regeneration, including processes such as remineralization and DNRA. When the net NH_4^+ flux is negative, the system displays net NH_4^+ uptake, including processes such as nitrification and N assimilation.

RESULTS

Concentration and %^{15}N Calibration Curves

There is strong agreement between the expected and observed ion counts for indophenol peaks when corrections for the ^{13}C effect and natural abundance of ^{15}N are taken into account (Figure 5). The peaks of interest (198.06 m/z, 199.06 m/z, and 200.06 m/z) are well-resolved, and there are no other substantial peaks within a similar m/z range that might interfere with the peaks of interest. These results confirm that we are able to detect the ^{15}N indophenol isotopic ratio from the MS chromatograms.

There is a linear response between total NH$_3$ concentration and absorbance at 495 nm ($R^2 = 0.9996$, $S_y = 9.15$, n = 12), and between expected %^{15}N and determined %^{15}N ($R^2 = 0.9997$, $S_y = 0.665$, n = 12) in a milli-Q water matrix (18 MΩ); (Figure 6). The slope of the %^{15}N curve was approximately equal to 1, which is a noteworthy component of this technique; there is very strong linear agreement between the expected %^{15}N from the standards and determined %^{15}N from the method, confirming that we are able to accurately measure the N isotope ratio, validating and the approach taken in this technique. The 1:1 relationship between expected %^{15}N and determined %^{15}N also indicates that no linear regression is necessary to standardize between the two values; %^{15}N can be determined directly from peak area ratios without calculating a calibration curve.

To ensure that the reaction and extraction process proceeds equivalently with both N isotopes, concentration standards were created with 99.6% ^{14}N-NH$_4^+$ (natural abundance) and 98% ^{15}N-NH$_4^+$ (manufacturer's purity). The resulting concentration calibration curves were visibly virtually identical, with the ^{14}N total [NH$_3$] curve (slope = 21.1±0.4; $S_y = 15.4$, n = 12) and the ^{15}N total [NH$_3$] curve (slope = 20.9±0.2 µM^{-1}; $S_y = 10.6$, n = 12) both demonstrating low mean standard deviation and similar slopes. Thus, this method does not promote measurable fractionation between the N isotopes.

The limit of detection is 1.5 µM for total NH$_3$ concentration and 2.2% ^{15}N in a milli-Q water matrix. The upper limit for concentration was not determined, but it is likely set by the capacity of the Sep-Pak column during extraction and the DAD upper limit.
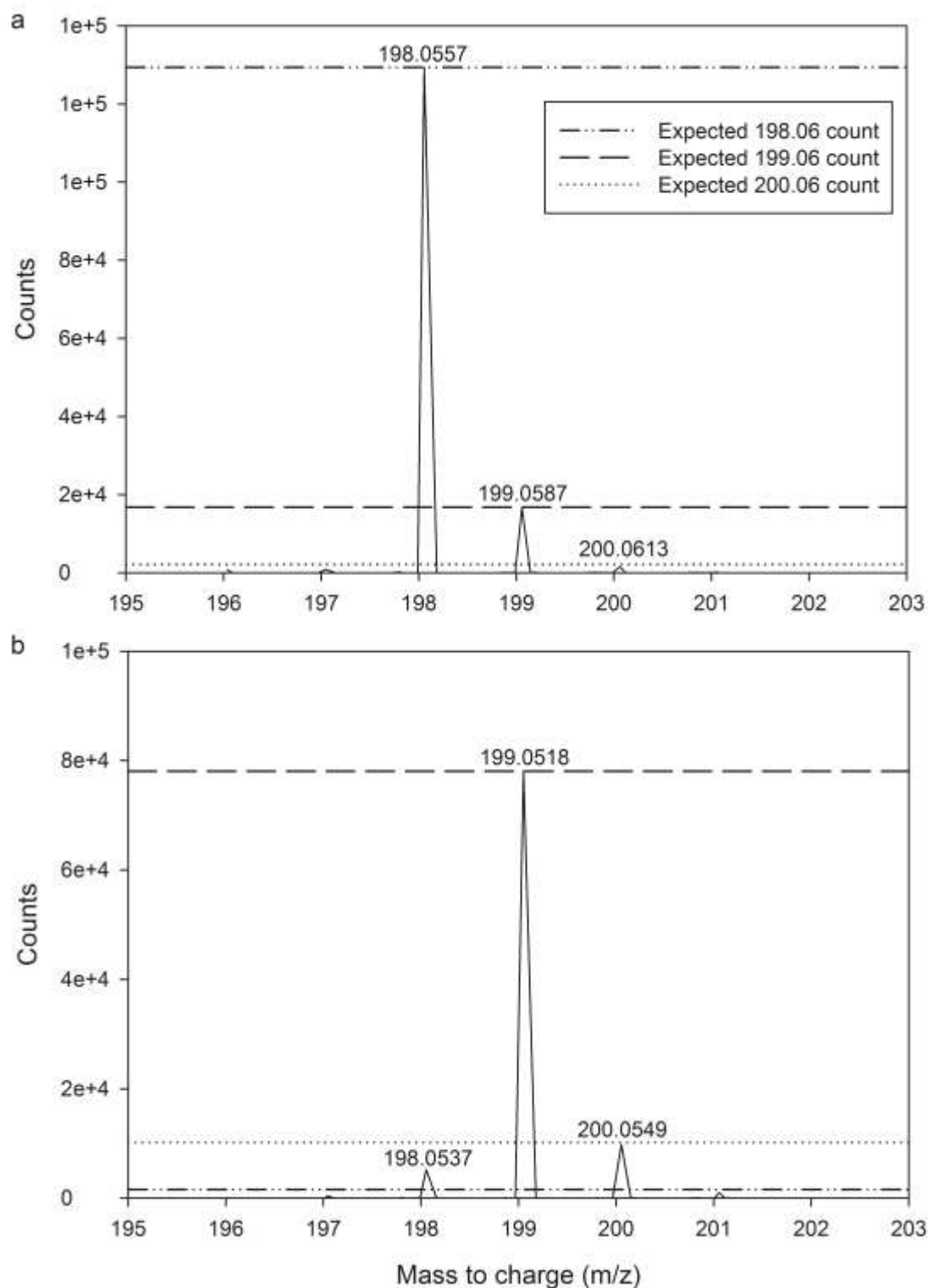
Figure 5. Spectral results in detected ion counts of standards containing 35 μM NH_4^+ and 99.6% ^{14}N-NH_4^+ (a) and 98% ^{15}N-NH_4^+ (b). The expected isotopic distribution of each species, normalized to the highest peak shown in each spectrum, is marked with horizontal dashed lines

17

Figure 6. Calibration curves in a milli-Q water (18 MΩ) matrix of absorbance at 495 nm vs. known standard total [NH_3] (n = 12) with %[15]N for each standard shown (a) and determined %[15]N vs. known standard %[15]N (n = 12) with total [NH_3] for each standard shown (b). Quadratic 99.9% confidence intervals are plotted in dashed grey.

18

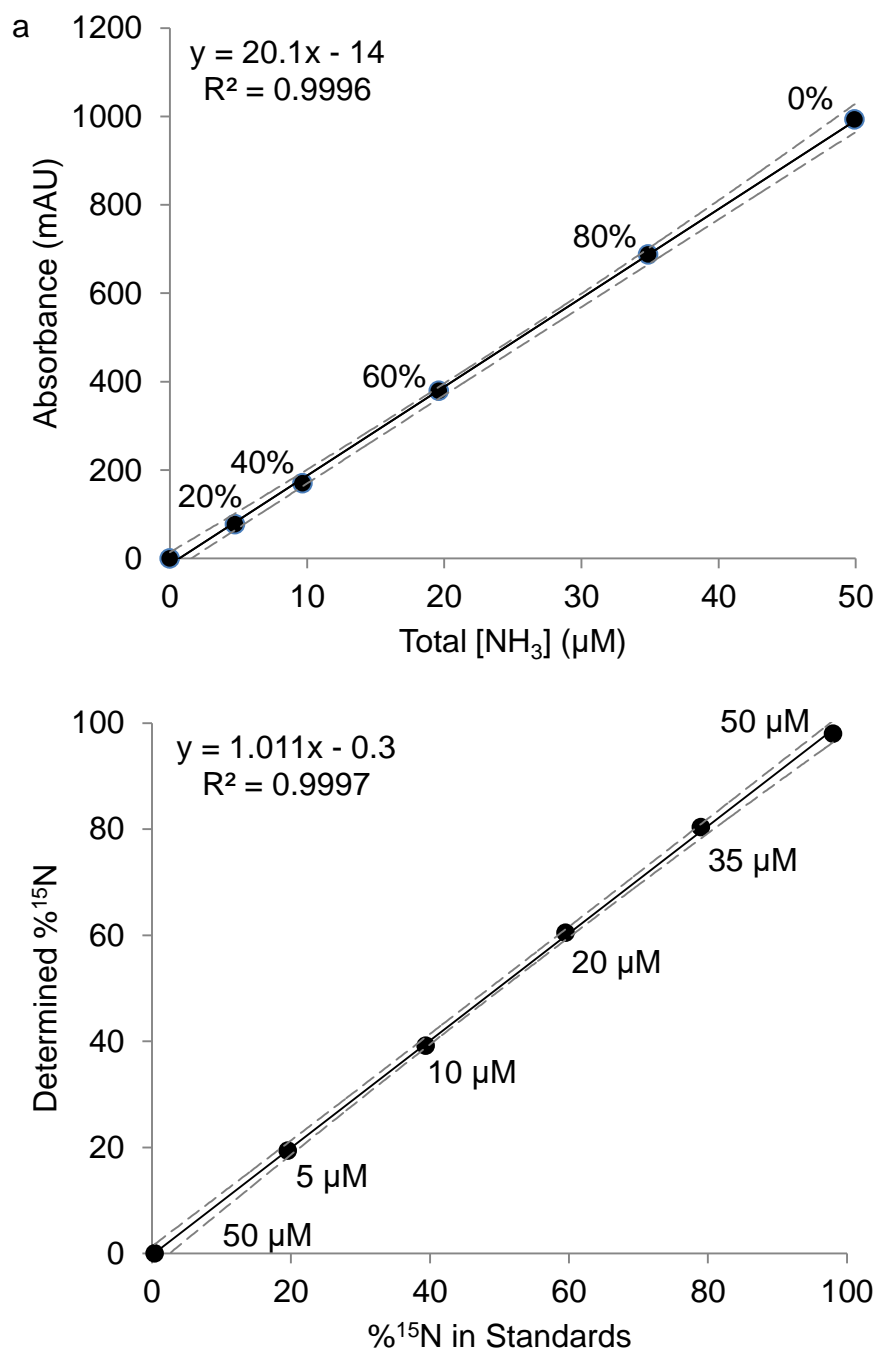The moderate total NH_3 concentration blanks (0.7 ± 0.3 μM) are likely due to NH_3 contamination from the air, glassware, and extraction process. Several measures were put in place to limit ammonium contamination, including limiting the sample's exposure to air, extra rinses of water or acetonitrile between each extraction step, and a longer run-time on the ESI-MS to prevent sample spill-over.

It is likely that the NH_3 concentration blank and the LODs for both the total $[NH_3]$ and $\%^{15}N$ calibration curve could be decreased by as much as an order of magnitude each if additional care against NH_3 contamination was taken in the sample preparation. For example, future standard curves could be prepared in a room separated from the main laboratory. This might prevent NH_3 contamination from a standard laboratory environment that freely utilizes NH_3-containing reagents and samples.

The mean standard deviations of the calibration curves do not substantially change when the amount of time the sample spent in the color formation stage of the procedure is varied from 6 hours to 7 days (Table 5), indicating that reaction time could be greater than 1 day as long as unknowns are analyzed with a calibration curve that has been reacted for the same amount of time.

DOC and Salinity Effects

When filtered water from a DOC-containing stream (6.69 mg DOC L^{-1}) was spiked with various NH_4^+ concentrations and isotope ratios, a linear relationship was observed for absorbance at 495 nm vs. total $[NH_3]$ ($\varepsilon' = 20.0\pm0.3$ mol mL^{-1} cm^{-1}, $R^2 = 0.9992$, $S_y =$

Table 5. Response of calibration curves in a milli-Q water matrix with varied color formation reaction times (n = 8). ε' is the effective molar absorptivity (mol mL^{-1} cm^{-1}) calculated from the slope of the calibration curve. The slope of the calibration curve is the ratio of determined $\%^{15}N$ to standard $\%^{15}N$.

Time Reacted	Total [NH₃]		%¹⁵N	
	ε'	S_y	Slope	S_y
6 hours	21.4±0.4	17.2	1.01±0.02	1.57
1 day	20.5±0.3	11.4	1.02±0.04	2.80
3 days	21.8±0.5	21.6	1.04±0.03	2.69
7 days	20.8±0.2	8.66	1.01±0.02	1.88

12.4, n = 12) and calculated $\%^{15}N$ vs. expected $\%^{15}N$ (slope = 1.00±0.02, R^2 = 0.9978, S_y = 1.77, n = 12). However, the DOC absorbance blank was not only due to total $[NH_3]$ contamination; the higher organic concentration of the matrix included unrelated DOC compounds that also absorb in the 495 nm wavelength range. Determination of the initial $[NH_4^+]$ present in the matrix is required to calculate the expected $\%^{15}N$ in the spike.

Spikes of a seawater sample (36‰) with various NH_4^+ concentrations and isotope ratios also displayed a linear relationship for absorbance at 495 nm vs. total $[NH_3]$ (ε' = 21.2±0.7 mol mL^{-1} cm^{-1}, R^2 = 0.9962, S_y = 27.0, n = 12) and calculated $\%^{15}N$ vs. expected $\%^{15}N$ (slope = 1.000±0.009, R^2 = 0.9997, S_y = 0.663, n = 12). To create calibration curves for unknown samples at salinity, we suggest processing standards in an artificial seawater matrix with a composition of NaCl salt at the desired salinity concentration and a bicarbonate buffer (0.196 g/L $NaHCO_3$) to approximate sample salinity. For a calibration curve with an artificial seawater matrix (19‰), a linear relationship and low mean standard error was displayed for absorbance at 495 nm vs. total $[NH_3]$ (R^2 = 0.9999, S_y = 2.63, n = 12) and determined $\%^{15}N$ vs. standard $\%^{15}N$ (R^2 = 0.9996, S_y = 0.818, n = 12); (Figure 7). This curve exhibited low limits of detection: 0.82 μM for NH_4^+ concentration and 2.7% ^{15}N.

Sample Stability

To test the stability of the indophenol extraction into acetonitrile, one calibration curve in an artificial seawater matrix (19‰) was analyzed by DAD and ESI-MS for 21 days. Over time, the determined $\%^{15}N$ of an extracted standard remained relatively consistent, while the absorbance at 495 nm generally increased as the days since the sample was extracted increased (Figure 8), possibly due to evaporation of the samples. The mean standard error of the total $[NH_3]$ calibration curve fit increases over time, while the mean standard error of the $\%^{15}N$ calibration curve fit showed no increase (Table 6). This increased standard error represents greater random error in the indophenol absorbance measurements as the time after extraction increased. However, the total $[NH_3]$ change appears to be relatively small, and should not affect unknown analysis as long as samples are processed at the same time as the calibration curve used.

20
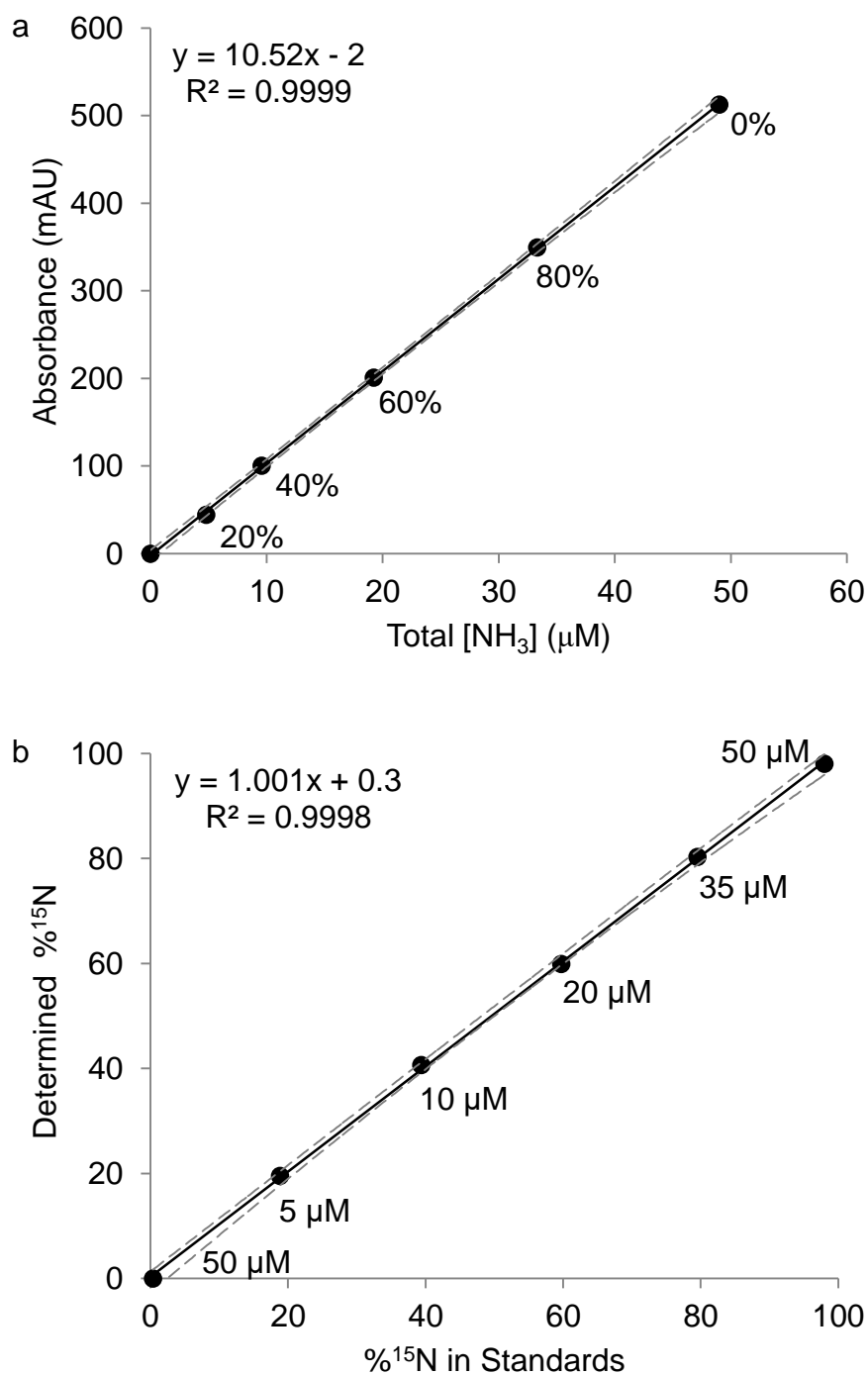
Figure 7. Calibration curves in an artificial seawater (19‰) matrix of absorbance at 495 nm vs. known standard total [NH_3] (n = 12) with %[15]N for each standard shown (a) and determined %[15]N vs. known standard %[15]N (n = 12) with total [NH_3] for each standard shown (b). Quadratic 99.9% confidence intervals are shown by dotted grey lines.

Figure 8. One standard (20 μM, 60%[15]N) run on a DAD and an ESI-MS multiple times over 21 days. Values are the averages of blank-corrected duplicates with standard deviations shown (n = 12). Note that the break in the y-axis serves to highlight variations in absorbance and determined %[15]N.

Table 6. Response of one calibration curve in an artificial seawater matrix (19‰) that was analyzed by DAD and ESI-MS 5 times over 21 days (n = 12). ε' is the effective molar absor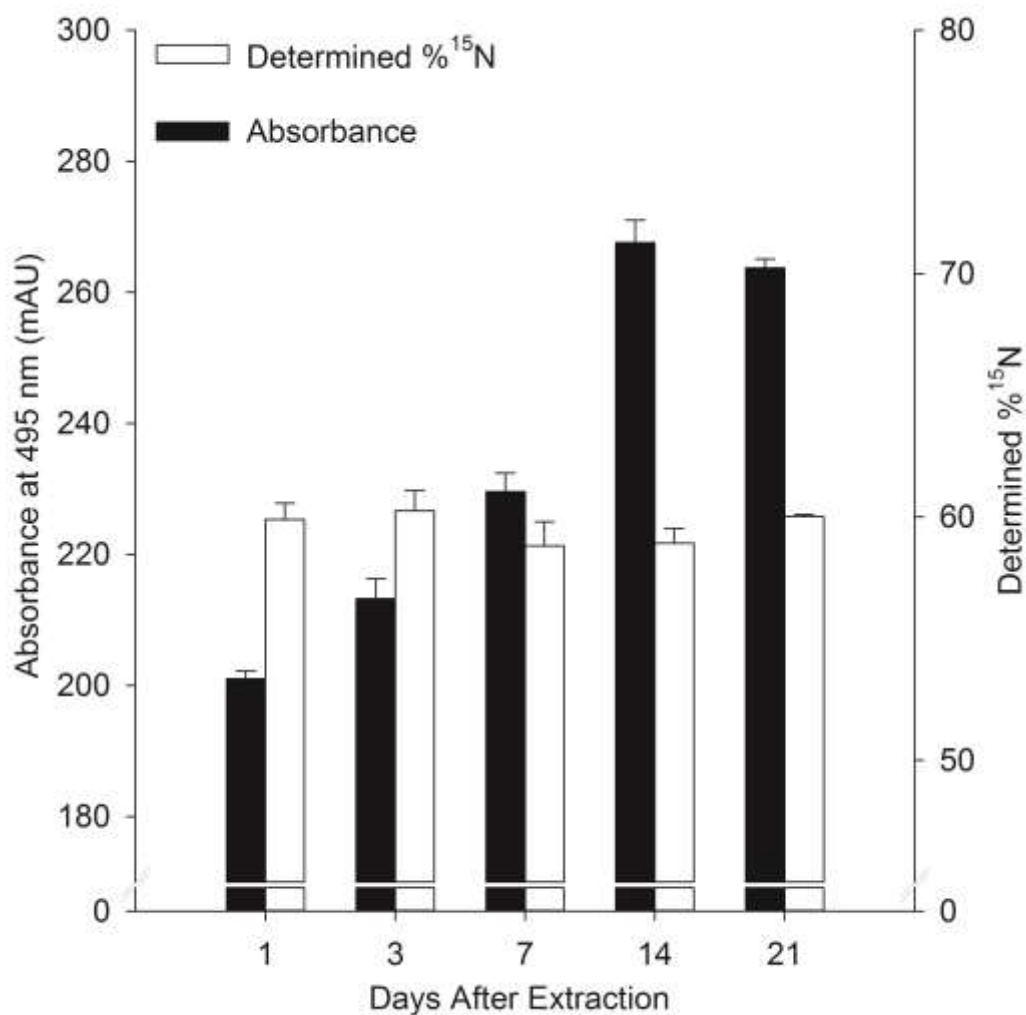ptivity (mol mL^{-1} cm^{-1}) calculated from the slope of the calibration curve. The slope of the calibration curve is the ratio of observed %^{15}N to actual %^{15}N.

Days After Extraction	Total [NH$_3$]		%^{15}N	
	ε'	S_y	Slope	S_y
1	10.52±0.06	2.63	1.01±0.01	0.82
3	10.96±0.09	3.91	1.01±0.02	1.32
7	11.7±0.1	4.77	1.009±0.009	0.62
14	13.5±0.2	10.0	1.001±0.008	0.69
21	14.9±0.4	15.5	1.006±0.009	0.72

Experimental Sample Results

To demonstrate the application of this method for analyzing sample outputs of ^{15}N tracer experiments, the results of sediment core incubation experiments from Mission River, TX, were analyzed using this novel technique. The net NH_4^+ flux and net ^{15}N-NH_4^+ flux were determined from 2 flow-through sediment core incubations (n = 4); (Figure 9) in order to examine rates of DNRA that occurred within the sediment core incubation.

Unfortunately, the results of this sediment incubation experiment were inconclusive, and a DNRA rate could not be accurately quantified due to a lack of ^{15}N enrichment of the NH_4^+ pool. The results suggest that multiple rapid N transformation processes occurred within the system.

In general, both cores show a net zero rate of NH_4^+ production, suggesting that uptake and regeneration processes are in balance. When the NH_4^+ flux rates are nonzero, there tends to be a positive net rate of NH_4^+ regeneration, indicating that there is net NH_4^+ production in the system, as would be expected from DNRA rates. The only exception is day 1 of the downstream core incubation (Figure 9.b), which shows high rates of total NH_4^+ uptake. This may be due to a lack of equilibrium conditions after the initial NO_3^- spike, and the days 2 and 3 are likely more accurate representations of the true net NH_4^+ flux.

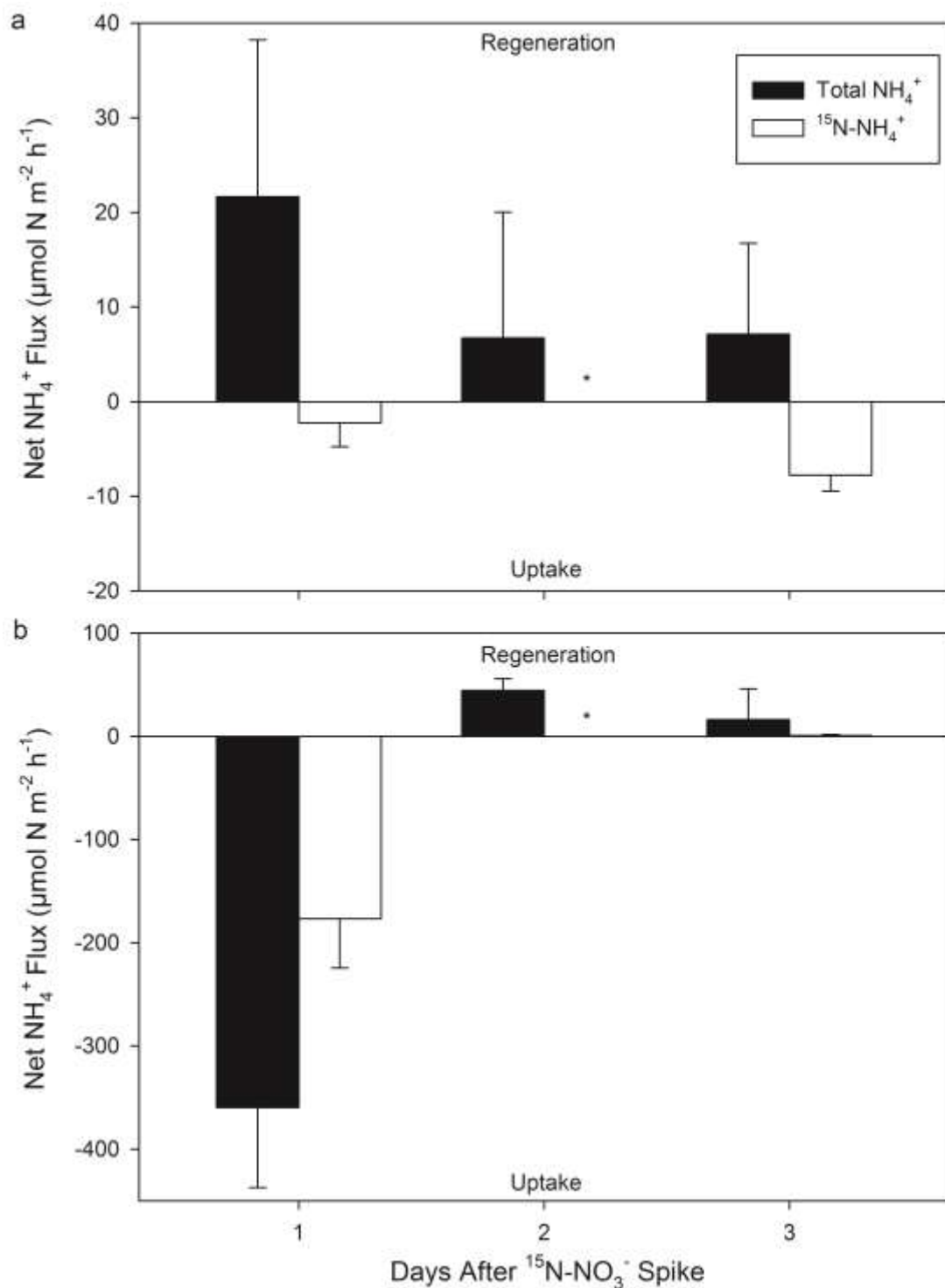Figure 9. Net NH_4^+ flux results of two soil core incubation experiments from an upstream site (a) and a downstream site (b) on Mission River, TX. Input water was spiked with $^{15}N\text{-}NO_3^-$ to measure the rate of N reduction to NH_4^+. Asterisks (*) represent measurements of 0% $^{15}N\text{-}NH_4^+$. Error bars represent standard deviations (n = 4). Note the difference in y-axis scales.

Although there is sometimes net NH_4^+ production, there is no strong ^{15}N-NH_4^+ production signal; all nonzero ^{15}N-NH_4^+ fluxes are negative, indicating a net ^{15}N uptake. This result suggests that DNRA is not a dominant process in the system, and the net production of NH_4^+ is not due to NO_3^- reduction, as with DNRA, but due to another N transformation such as remineralization. A dominant remineralization process would produce a positive net flux of total NH_4^+, but would not produce ^{15}N-NH_4^+ from the ^{15}N-NO_3^- pool.

Finally, it appears as though the NH_4^+ is cycling quickly through the system, as evidenced by the dilution of the ^{15}N signal over time. The NH_4^+ present in the system was in high demand, and most molecules were likely consumed soon after production. The ^{15}N tracer spiked into the system was being cycled quickly through different N species and was subsequently diluted through the course of the experiment. The N transformations responsible for this dilution interfere with our ability to quantify even a low DNRA rate because the [^{15}N-NH_4^+] signal required to calculate the rate is depleted by these other processes.

If positive DNRA rates were present within the sediment core incubation, they were obscured by other N processes within the sediment core. These processes, which likely included remineralization from organic N, occurred at a finer time-scale than experimental sampling took place, preventing us from capturing the dynamic N processes taking place within the core incubations. If output sampling had occurred more frequently than once every 24 h, we may have been able to observe the DNRA process before the [^{15}N-NH_4^+] was diluted by subsequent N transformations.

A portion of the samples generated in this experiment were also analyzed via the AIRTS/HPLC method for ^{15}N-NH_4^+ determination (W. S. Gardner, personal communication). In general, there was good agreement between the two methods. The inconclusive results of this study are due set-backs in the incubation experiment itself, and not in the analysis of the sample outputs by the method presented in this paper.

DISCUSSION

Method Evaluation

We have developed a novel technique to determine NH_4^+ concentration and isotopic ratios from ^{15}N tracer experiments that is easy to use, time-effective, has a low detection limit, and uses small sample volumes. This method extends ^{15}N-NH_4^+ analysis to ESI-MS instrumentation, which has never been previously accomplished. Additionally, this method is accessible to undergraduate institutions because the instrumentation required includes only a spectrophotometer and a mass spectrometer that is compatible with an ESI input, both relatively common instruments in an undergraduate facility. Thus, this method is broadly accessible and expands the ability for N researchers to perform and analyze ^{15}N-tracer experiments.

This technique is more convenient that many other ^{15}N methods. A 3 mL sample volume allows researchers to collect smaller, more easily transportable volumes of sample and still have some volume left over for additional water sampling tests. This is especially important for flow-through sediment core experiments, where sampling the outflow water in large volumes takes a considerable amount of time because of the low flow rate of the experiment. The simultaneous determination of UV-Vis and MS analysis provides simultaneous determination of NH_4^+ concentration along with isotopic analysis, which reduces analysis time and sample volume necessary to compute N-transformation rates. The technique can be used for freshwater, saltwater, and DOC-containing samples, allowing for a broad range of experimental applications, including freshwater streams and lakes, estuaries, and marine ecosystems. Additionally, the automation provided by the LabView software can process large quantities of samples (~50-100 per day), and the SASE can be employed and adjusted to accommodate specific needs. The LabView software uses an intuitive visual programing language, and the SASE "dashboard" coding is simple to use and adjust.

This technique is not limited to NH_4^+; nitrate (NO_3^-) and nitrite (NO_2^-) can be complexed into an azo dye (mass 369.12 or 370.12 m/z) via the Griess reaction, a traditional colorimetric reaction used for concentration determination (Miranda et al. 2001). Although a different elution procedure would be necessary for the solid-phase

extraction of the Griess azo dye, the method would follow a parallel concept as the NH_4^+ indophenol method.

Phenol is a known carcinogen and can be hazardous if it is inhaled, ingested, or comes into contact with skin. This method was adjusted to use lower levels of phenol reagent than in previous methods for measuring NH_4^+ concentrations, therefore decreasing exposure and the amount of hazardous waste produced.

While this method is well-suited to analyze the sample output of ^{15}N tracer experiments where a relatively large amount of ^{15}N species is added to the experimental system, this method is not suitable for ^{15}N natural abundance experiments. Many N researchers are interested in measuring the natural levels of ^{15}N present in different environments or organisms, but such small deviations in the abundance of the ^{15}N isotope cannot be determined with the ESI-MS in this method. This is because typical ESI-MS instruments, such as the TOF instrument used in this study, do not have the signal-to-noise resolution required for %^{15}N determination to the hundredth of a percent. Tracer experiment samples generally contain larger difference in %^{15}N and tend to be well within the suitable range for this method.

Applications to ^{15}N Tracer Experiments

The tracer experiment application presented in this paper was not successful in calculating rates of DNRA in soil core incubation experiments. The results of the study were inconclusive because multiple N transformation processes occurred at a faster rate than our sampling timescale was able to capture. This led to much of the ^{15}N-NH_4^+ formed via DNRA to be transformed into another N species before we could successfully capture the NH_4^+ species and measure the rate of DNRA transformation.

To better design this sediment core experiment, we recommend that the outflow water be sampled more frequently than every 24 hours, perhaps every 6 hours. This would provide a finer scale to observe N transformations, and possibly capture the elusive DNRA rate.

Despite the lack of conclusive results from this experiment, this method is currently being employed to analyze samples from other ^{15}N tracer experiments, including in estuary and lake environments (D. A. Bruesewitz, personal communication). The use of

this method has proved to be efficient and effective in the determination of N transformation rates from ^{15}N tracer experiment samples.

Planned Future Experiments

Future experiments should be conducted to more conclusively verify this method (Table 7). These studies should include additional testing to determine a more accurate limit of detection for total [NH$_3$] and %^{15}N using the milli-Q water calibration curve. We predict that the true limit of detection of this method is at least an order of magnitude smaller than the limit presented here. To verify this, future standard curves should be prepared with care in a NH$_3$ "clean room", in which significant concentrations of NH$_3$, NH$_4^+$, or other N species have not been routinely used in the laboratory space. Hopefully, these precautions will prevent NH$_3$ contamination from a standard laboratory environment and decrease the standard error and NH$_3$ blank concentrations in the calibration curve.

Other future experiments should test if increasing the volume of initial sample will increase the sensitivity of the instrument. Sample volumes of 1-10 mL could be tested to determine how the mean standard error and limit of detection varies with sample volume. At the moment, the low sample volume used in this method is a logistical advantage, but increasing the volume may increase the signal detected by the instruments, which would in turn lower the standard error and limit of detection for the method. If this is the case, researchers could decide for themselves how to manage the trade-off between the logistical ease of lower sample volumes and the increased sensitivity of larger sample volumes.

Additional testing should also optimize the determination of ^{15}N-NH$_4^+$ in water containing concentrations of DOC. Samples containing a substantial concentration of DOC were observed to contain organic compounds other than indophenol that absorb at 495 nm. To correct for this absorbance interference, it may be possible to increase the pH to convert the indophenol to its blue, deprotonated form, which absorbs at 628 nm. Fewer DOC compounds are likely to absorb in the higher wavelength, and so there would be less interference in the indophenol absorbance signal. It might also be possible to increase the amount of phenol reagent used, in case a portion of the phenol added to the color

28

Table 7. Planned future experiments for method validation.

	Question	Design
1	What is the true LOD of this method?	Test additional calibration curves with a milli-Q water (18 MΩ) matrix, taking extra precautions with laboratory NH_3 contamination.
2	How does the method's sensitivity change with sample volume?	Alter initial sample volume from 1-10 mL and examine the calibration curve response.
3	How does the method's sensitivity change with injection volume?	Alter DAD and ESI-TOF injection volume from 5-50 μL and examine the calibration curve response.
4	How can samples with high DOC levels be processed most accurately and effectively?	a. Increase sample pH after extraction to determine absorbance spectrum of indophenol blue at 628 nm. b. Increase the amount of phenol reagent used to ensure complete complexation of total NH_3. c. Use the total ion count of all indophenol species to estimate total $[NH_3]$, instead of using UV-Vis spectrophotometry.

formation reaction is reacting with the DOC molecules. Increasing the amount of phenol reagent would then ensure all NH_3 molecules present in the sample are reacted into phenol. Finally, the total ion count for all indophenol species (198.06, 199.06, and 200.06 m/z chromatograms) could be used to estimate $[NH_4^+]$. The isotopic ratio of indophenol should be unaffected by the DOC concentration, and can be calculated as normal.

CONCLUSION

The method for the determination of NH_4^+ isotope ratios from ^{15}N tracer experiments outlined in this paper extends the ability for researchers to study the N cycle by preforming and analyzing the results of ^{15}N tracer experiments. The technique is accessible, flexible, time-effective, and has a low sample volume. It extends the analysis of ^{15}N-NH_4^+ to ESI-MS instruments, thus expanding the ability of N researchers to conduct such tracer experiments with a wider range of instrumentation.

The method presented has low standard error and a low limit of detection for both fresh (1.5 μM NH_4^+, 2.2% ^{15}N) and saltwater (0.82 μM NH_4^+, 2.7% ^{15}N) matrixes, and the true limit of detection is likely lower. The method can be extended to account for samples with concentrations of DOC, and is stable for at least 3 weeks in its extracted form.

The goal of this work was to facilitate environmental monitoring of N processes and anthropogenic perturbations in the N cycle in terrestrial, freshwater, and marine ecosystems. However, this method could have far-reaching implications in other fields as well. Disciplines such as biochemistry and atmospheric chemistry also use ^{15}N tracer experiments to track N transformations, and could adapt this technique for NH_4^+ isotopic determination in a broad range of samples.

PERSONAL COMMUNICATION

Zachary Mondschein, Colby College, Chemistry and Environmental Studies Research Assistant.

Wayne S. Gardner, University of Texas Marine Science Institute, Professor Emeritus: Department of Marine Science.

Denise A. Bruesewitz, Colby College, Assistant Professor of Environmental Studies.

LITERATURE CITED

Alexander, R. B., J. K. Bohlke, E. W. Boyer, M. B. David, J. W. Harvey, P. J. Mulholland, S. P. Seitzinger, C. R. Tobias, C. Tonitto, and W. M. Wollheim. 2009. Dynamic modeling of nitrogen losses in river networks unravels the coupled effects of hydrological and biogeochemical processes. Biogeochemistry 93:91–116.

Alexander, R. B., R. A. Smith, G. E. Schwarz, E. W. Boyer, J. V Nolan, and J. W. Brakebill. 2008. Differences in phosphorus and nitrogen delivery to the Gulf of Mexico from the Mississippi River Basin. Environmental Science and Technology 42:822–830.

Brooks, P. D., J. M. Stark, B. B. McInteer, and T. Preston. 1989. Diffusion method to prepare soil extracts for automated nitrogen-15 analysis. Soil Science Society of America 53:1707–1711.

Bruesewitz, D. A., W. S. Gardner, R. F. Mooney, and E. J. Buskey. 2015. Seasonal water column NH_4^+ cycling along a semi-arid sub-tropical river – estuary continuum: responses to episodic events and drought conditions. Ecosystems 18:792–812.

Bruesewitz, D. A., J. L. Tank, and S. K. Hamilton. 2012. Incorporating spatial variation of nitrification and denitrification rates into whole-lake nitrogen dynamics. Journal of Geophysical Research 117:1–12.

Burgin, A. J., and S. K. Hamilton. 2007. Have we overemphasized the role of denitrification in aquatic ecosystems? A review of nitrate removal pathways. Frontiers in Ecology and the Environment 5:89–96.

Carini, S. A., and S. B. Joye. 2008. Nitrification in Mono Lake, California: Activity and community composition during contrasting hydrological regimes. Limnology and Oceanography 53:2546–2557.

Carpenter, S. R., N. F. Caraco, D. L. Correll, R. W. Howarth, A. N. Sharpley, and V. H. Smith. 1998. Nonpoint pollution of surface waters with phosphorus and nitrogen. Ecological Applications 8:559–568.

Clark, D. R., T. W. Fileman, and I. Joint. 2006. Determination of ammonium regeneration rates in the oligotrophic ocean by gas chromatography/mass spectrometry. Marine Chemistry 98:121–130.

Delwiche, C. C. 1977. Energy relations in the global nitrogen cycle. Ambio 6:106–111.

Diaz, R. J., and R. Rosenberg. 2008. Spreading dead zones and consequences for marine ecosystems. Science 321:926–930.

Dodds, W. K., V. H. Smith, and K. Lohman. 2002. Nitrogen and phosphorus relationships to benthic algal biomass in temperate streams. Canadian Journal of

Fisheries and Aquatic Sciences 59:865–874.

Dudek, N., M. A. Brzezinski, and P. A. Wheeler. 1986. Recovery of ammonium nitrogen by solvent extraction for the determination of relative ^{15}N abundance in regeneration experiments. Marine Chemistry 18:59–69.

Galloway, J. N., J. D. Aber, J. W. Erisman, S. P. Seitzinger, R. W. Howarth, E. B. Cowling, and B. J. Cosby. 2003. The nitrogen cascade. BioScience 53:341–356.

Gardner, W. S., H. A. Bootsma, C. Evans, and P. A. St. John. 1995. Improved chromatographic analysis of ^{15}N:^{14}N ratios in ammonium or nitrate for isotope addition experiments. Marine Chemistry 48:271–282.

Gardner, W. S., L. R. Herche, P. A. St. John, and S. P. Seitzinger. 1991. High-performance liquid chromatographic determination of ^{15}NH$_4$:[^{14}NH$_4$ + ^{15}NH$_4$] ion ratios in seawater for isotope dilution experiments. Analytical Chemistry 63:1838–1843.

Gardner, W. S., M. J. McCarthy, S. An, D. Sobolev, K. S. Sell, and D. Brock. 2006. Nitrogen fixation and dissimilatory nitrate reduction to ammonium (DNRA) support nitrogen dynamics in Texas estuaries. Limnology and Oceanography 51:558–568.

Glibert, P. M., J. Harrison, C. Heil, and S. Seitzinger. 2006. Escalating worldwide use of urea – a global change contributing to coastal eutrophication. Biogeochemistry 77:441–463.

Glibert, P. M., R. Maranger, D. J. Sobota, and L. Bouwman. 2014. The Haber Bosch – harmful algal bloom (HB – HAB) link. Environmental Research Letters 9.

Groffman, P. M., M. A. Altabet, J. K. Bohlke, K. Butterbach-Bahl, M. B. David, M. K. Firestone, E. Giblin, Anne, T. M. Kana, L. P. Nielsen, and M. A. Voytek. 2006. Methods for measuring denitrification: diverse approaches to a difficult problem. Ecological Applications 16:2091–2122.

Harris, D. C. 2010. Quantitative chemical analysis. 8th ed. W. H. Freeman and Company, New York.

Holmes, R. M., J. W. McClelland, D. M. Sigman, B. Fry, and B. J. Peterson. 1998. Measuring 15-NH$_4^+$ in marine, estuarine and fresh waters: An adaptation of the ammonia diffusion method for samples with low ammonium concentrations. Marine Chemistry 60:235–243.

Howarth, R. W., G. Billen, D. Swaney, A. Townsend, N. Jaworski, K. Lajtha, J. A. Downing, R. Elmgren, N. Caraco, T. Jordan, F. Berendse, J. Freney, V. Kudeyarov, P. Murdoch, and Z. Zhao-Liang. 1996. Regional nitrogen budgets and riverine N & P fluxes for the drainages to the North Atlantic Ocean: Natural and human Influences. Biogeochemistry 35:75–139.

Johnston, A. M., C. M. Scrimgeour, H. Kennedy, and L. L. Handley. 2003. Isolation of ammonium-N as 1-sulfonato-iso-indole for measurement of δ^{15}N. Rapid Communications in Mass Spectrometry 17:1099–1106.

Liu, D., Y. Fang, Y. Tu, and Y. Pan. 2014. Chemical method for nitrogen isotopic analysis of ammonium at natural abundance. Analytical Chemistry 86:3787–3792.

McCarthy, M. J., S. E. Newell, S. A. Carini, and W. S. Gardner. 2015. Denitrification dominates sediment nitrogen removal and is enhanced by bottom-water hypoxia in the northern Gulf of Mexico. Estuaries and Coasts 38:2279–2294.

Miranda, K. M., M. G. Espey, and D. A. Wink. 2001. A rapid, simple spectrophotometric method for simultaneous detection of nitrate and nitrite. Nitric Oxide: Biology and Chemistry 5:62–71.

Mooney, R. F., and J. W. McClelland. 2012. Watershed export events and ecosystem responses in the Mission-Aransas National Estuarine Research Reserve, South Texas. Estuaries and Coasts 35:1468–1485.

Nolan, B. T., B. C. Ruddy, K. J. Hitt, and D. R. Helsel. 1997. Risk of nitrate in groundwaters of the United States - A national perspective. Environmental Science and Technology 31:2229–2236.

Paerl, H. W., J. T. Scott, M. J. Mccarthy, S. E. Newell, W. S. Gardner, K. E. Havens, D. K. Ho, S. W. Wilhelm, and W. A. Wurtsbaugh. 2016. It takes two to tango: When and where dual nutrient (N & P) reductions are needed to protect lakes and downstream ecosystems. Environmental Science and Technology 50:10805−10813.

Patton, C. J., and S. R. Crouch. 1977. Spectrophotometric and kinetics investigation of the Berthelot reaction for the determination of ammonia. Analytical Chemistry 49:464–469.

Peterson, B. J., W. M. Wollheim, P. J. Mulholland, J. R. Webster, J. L. Meyer, J. L. Tank, E. Marti, W. B. Bowden, H. M. Valett, A. E. Hershey, W. H. Mcdowell, W. K. Dodds, S. K. Hamilton, S. Gregory, and D. D. Morrall. 2001. Control of nitrogen export from watersheds by headwater streams. Science 292:86–90.

Preston, T., S. Bury, M. Presing, G. Moncoiffe, and C. Slater. 1996. Isotope dilution analysis of combined nitrogen in natural waters: I. Ammonium. Rapid Communications in Mass Spectrometry 10:959–964.

Rabalais, N. N., R. E. Turner, and W. J. Wiseman. 2002. Gulf of Mexico hypoxia, A.K.A. "The Dead Zone." Annual Review of Ecology and Systematics 33:235–263.

Rockstrom, J., W. Steffen, K. Noone, E. Lambin, T. M. Lenton, M. Scheffer, C. Folke, H. J. Schellnhuber, C. A. De Wit, T. Hughes, S. Van Der Leeuw, H. Rodhe, P. K. Snyder, R. Costanza, U. Svedin, M. Falkenmark, L. Karlberg, R. W. Corell, V. J. Fabry, J. Hansen, B. Walker, D. Liverman, K. Richardson, P. Crutzen, and J. Foley.

2009. Planetary Boundaries : Exploring the Safe Operating Space for Humanity. Ecology and Society 14.

Rupert, M. G. 2008. Decadal-scale changes of nitrate in ground water of the United States, 1988-2004. Journal of Environmental Quality 37:S240–S248.

Solorzano, L. 1969. Determination of ammonia in natural waters by the phenolhypochlorite method. Limnology and Oceanography 14:799–801.

Sorensen, P., and E. S. Jensen. 1991. Sequential diffusion of ammonium and nitrate from soil extracts to a polytetrafluoroethylene trap for ^{15}N determination. Analytica Chimica Acta 252:201–203.

Spalding, R. F., and M. E. Exner. 1993. Occurrence of nitrate in groundwater - A review. Journal of Environmental Quality 22:392–402.

Strange, C. F., O. Spott, B. Apelt, and R. W. Russow. 2007. Automated and rapid online determination of ^{15}N abundance and concentration of ammonium, nitrite, or nitrate in aqueous samples by the SPINMAS technique. Isotopes in Environmental and Health Studies 43:227–236.

Velinsky, D. J., J. R. Pennock, J. H. Sharp, L. A. Cifuentes, and M. L. Fogel. 1989. Determination of the isotopic composition of ammonium-nitrogen at the natural abundance level from estuarine waters. Marine Chemistry 26:351–361.

Vitousek, P. M., J. D. Aber, R. W. Howarth, G. E. Likens, A. Matson, D. W. Schindler, W. H. Schlesinger, and D. G. Tilman. 1997. Human alteration of the global nitrogen cycle: Sources and consequences. Ecological Applications 7:737–750.

Wymore, A. S., A. A. Coble, B. Rodríguez-Cardona, and W. H. Mcdowell. 2016. Nitrate uptake across biomes and the influence of elemental stoichiometry: A new look at LINX II. Global Biogeochemical Cycles 30:1183–1191.

Zhang, L., M. A. Altabet, T. Wu, and O. Hadas. 2007. Sensitive measurement of NH_4^+ ^{15}N/^{14}N ($\delta^{15}NH_4^+$) at natural abundance levels in fresh and saltwaters. Analytical Chemistry 79:5589–5595.
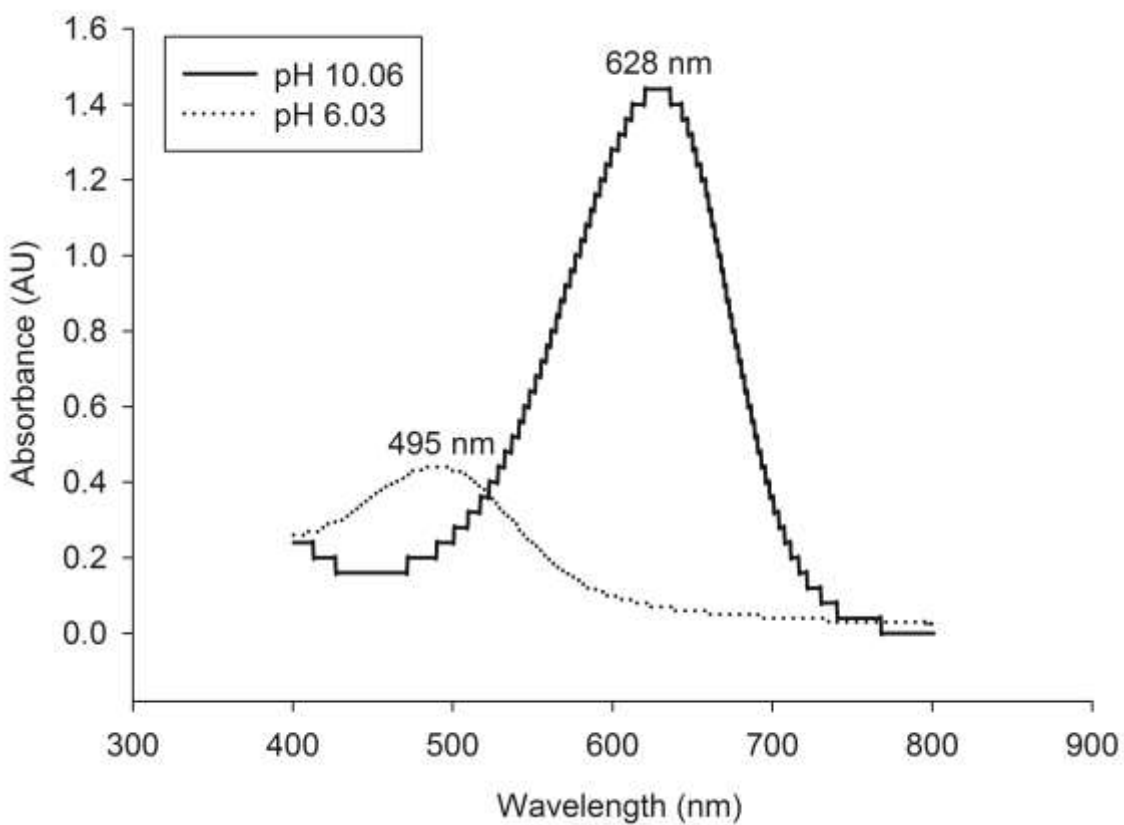
APPENDIX

Figure A.1. Absorbance spectrum of indophenol in solutions at two different pH values. The "blue" deprotonated solution absorbs at ~628 nm and the "red" protonated solution absorbs at ~495 nm.
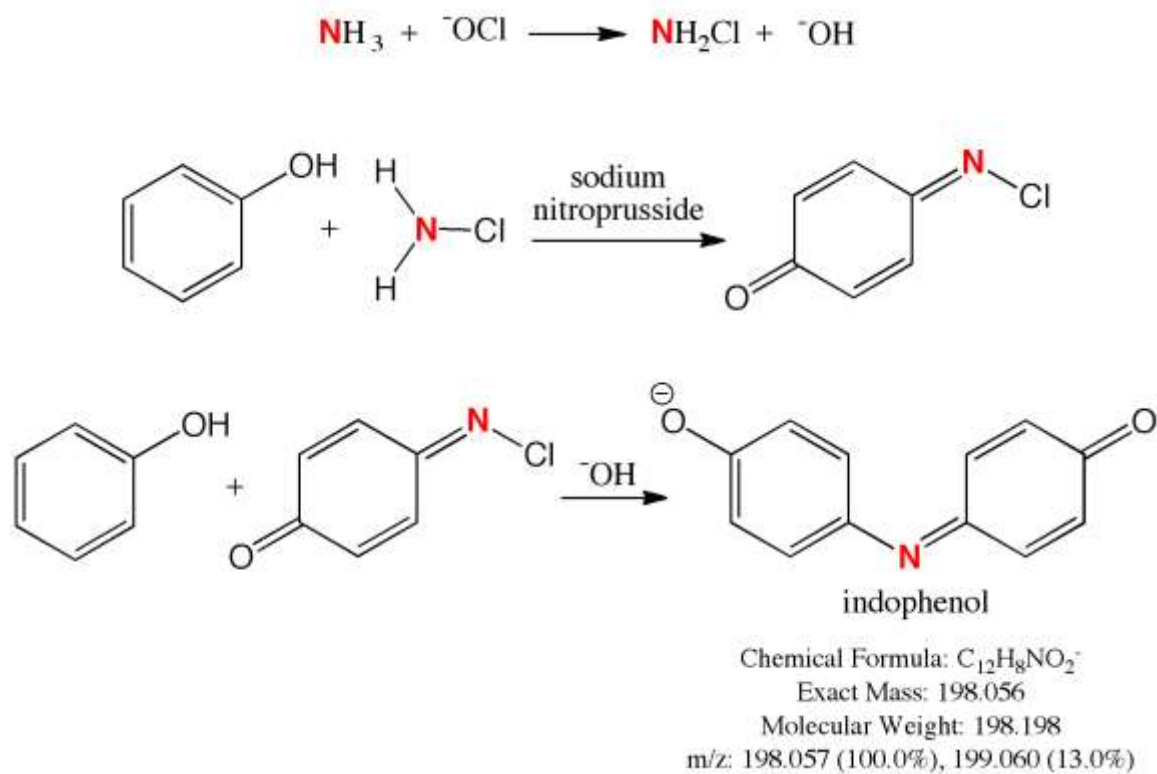
Figure A.2. Mechanism for the formation of deprotonated indophenol. The N atom is either ^{14}N or ^{15}N. Adapted from Patton and Crouch (1997).